PNAS RESEARCH ARTICLE | EARTH, ATMOSPHERIC, AND PLANETARY SCIENCES

Dominance of felsic continental crust on Earth after 3 billion years ago is recorded by vanadium isotopes

Shengyu Tian[a,b,1], Xin Ding[a,b,1], Yuhan Qi[a], Fei Wu[c], Yue Cai[d,e], Richard M. Gaschnig[f], Zicong Xiao[a], Weixin Lv[a], Roberta L. Rudnick[g,h,2], and Fang Huang[a,b,2]

Contributed by Roberta L. Rudnick; received December 5, 2022; accepted February 8, 2023; reviewed by Peter A. Cawood and Julie Prytulak

The transition from mafic to felsic upper continental crust (UCC) is crucial to habitability of Earth, and may be related to the onset of plate tectonics. Thus, defining when this crustal transition occurred has great significance for the evolution of Earth and its inhabitants. We demonstrate that V isotope ratios (reported as $\delta^{51}V$) provide insights into this transition because they correlate positively with SiO_2 and negatively with MgO contents during igneous differentiation in both subduction zones and intraplate settings. Because $\delta^{51}V$ is not affected by chemical weathering and fluid–rock interactions, $\delta^{51}V$ of the fine-grained matrix of Archean to Paleozoic (3 to 0.3 Ga) glacial diamictite composites, which sample the UCC at the time of glaciation, reflect the chemical composition of the UCC through time. The $\delta^{51}V$ values of glacial diamictites systematically increase with time, indicating a dominantly mafic UCC at ~3 Ga; the UCC was dominated by felsic rocks only after 3 Ga, coinciding with widespread continental emergence and many independent estimates for the onset of plate tectonics.

continental crust | glacial diamictite | vanadium isotopes | crustal evolution

Significance

Earth's earliest crust may have been basaltic by analogy with the ancient crusts of Mercury, Venus, and Mars. On Earth, the timing of the transition from mafic crust to felsic continental crust may have influenced continental emergence, the rise of atmospheric oxygen, the start of plate tectonics, and habitability. However, this timing is currently debated. New V isotope data for the fine-grained matrix of lithified glacial tills, deposited between 3000 to 350 Mya, indicate that the exposed crust was dominantly mafic early on and became more felsic in the post-Archean. These observations are free of the ambiguity seen in previous isotopic proxy studies and provide a reliable assessment of the compositional evolution of the upper continental crust.

Earth has a bimodal topography, reflecting two types of crust with distinct lithologies. Basaltic crust, covering ~60% surface of the Earth, mostly lies below sea level and forms the young (<200 Ma) ocean floor. By contrast, continental crust is more felsic, forming the buoyant, high-standing, and more ancient continents. Within our solar system, this crustal duality is unique to Earth and is a direct manifestation of the operation of plate tectonics, which is widely considered to generate felsic continental crust (1–3). The dominance of felsic continental crust is crucial to planetary habitability, as the transition from mafic to felsic crust may have impacted atmospheric composition, climate stabilization, and nutrient supplies to the oceans (4–6). Thus, determining when the emerged crust transitioned from mafic to felsic is critical in understanding the evolution of our planet (2, 3).

While early initiation of plate tectonics (~3.5 to 3.25 Ga) has been inferred by some studies (2, 7, 8), others suggest its initiation, and hence the generation of dominantly felsic continental crust, only commencing in the late Archean (3.0 to 2.5 Ga) (3, 9–12). Reconstructing the composition of ancient upper continental crust (UCC) has relied heavily on the use of trace element proxies in terrigenous sedimentary rocks such as shales, which provide averages of large areas of the continental surface. However, such proxies have been interpreted in diametrically opposite ways (change in crust composition, vs. no change) depending on the trace element(s) and ratios under consideration (3, 7, 8, 10, 12, 13). It is thus important to establish a reliable tracer to discriminate mafic and felsic crustal components and apply this tracer to reconstruct the composition of the UCC throughout Earth's history. Vanadium (V) stable isotopes provide such an opportunity.

Here we show that V isotope data in terrigenous sedimentary rocks are an unambiguous proxy for the major element composition of the upper continental crust. Under the redox conditions of Earth, V is mainly present as V^{3+}, V^{4+} or V^{5+}, in oxides or silicate melts with negligible amount of V^{2+}. Theoretical and experimental studies show that crystallographic sites with higher coordination number, or which contain elements with lower valence states, preferentially incorporate the lighter isotope of V (14–17). For example, V^{4+} and V^{5+} enter into fourfold and fivefold coordination with oxygen in silicate melts, whereas V^{3+} and V^{4+} tend to enter octahedral (sixfold) coordination sites within pyroxene and Fe-Ti oxides (18–20). During magmatic differentiation, V isotopic compositions become progressively heavier with increasing crystallization, as is the case with Ti isotopes (14–17, 21–24). However, stable Ti isotope compositions of igneous rocks show two distinct trends with magmatic differentiation: Intraplate ocean island lavas have significantly higher $^{49}Ti/^{47}Ti$ than subduction-related lavas at the same MgO or SiO_2 contents (21–23). This probably relates to the much higher TiO_2 contents and more Fe-Ti oxide crystallization in the ocean island lavas than subduction zone lavas. By contrast, because the variations of V contents in the two suites of igneous rocks are similar (*SI Appendix*, Fig. S1), their

Author contributions: R.M.G., R.L.R., and F.H. designed research; S.T., X.D., F.W., and W.L. performed research; S.T., X.D., Y.Q., and F.H. contributed new reagents/analytic tools; S.T., X.D., Z.X., R.L.R., and F.H. analyzed data; Y.C. and R.L.R. provided samples; R.M.G. characterized samples; and S.T., X.D., Y.C., R.M.G., R.L.R., and F.H. wrote the paper.

Reviewers: P.A.C., Monash University; and J.P., Durham University.

The authors declare no competing interest.

[1]S.T. and X.D. contributed equally to this work.

[2]To whom correspondence may be addressed. Email: rudnick@geol.ucsb.edu or fhuang@ustc.edu.cn.

This article contains supporting information online at https://www.pnas.org/lookup/suppl/doi:10.1073/pnas.2220563120/-/DCSupplemental.

Published March 9, 2023.

V isotope fractionation patterns are indistinguishable (*SI Appendix*, Supplementary Text-SOM.3).

To document V isotopic behavior during magma differentiation, we analyzed forty-six subduction-related igneous rocks from the Kamchatka, Southern Lesser Antilles, and Aleutian intraoceanic island arcs. These rocks have chemical compositions encompassing the entire range of global calc-alkaline rocks from subduction zones (*SI Appendix*, Figs. S1–S3 and Table S1). We also analyzed 24 composites of the fine-grained matrices of glacial diamictites from multiple continents with depositional ages of ~2.9, 2.4 to 2.2, 0.75 to 0.58, and ~0.3 Ga (*SI Appendix*, Fig. S4 and Table S2). These composites were generated by combining multiple (~120) diamictite samples from the same formations and have been used to constrain the compositional evolution of the UCC through time (12, 25–36) because glacial diamictites are unsorted sedimentary rocks and experienced much weaker syndepositional and postdepositional chemical weathering compared with other terrigenous sedimentary rocks such as shales and loess (25, 27, 37). Finally, to conduct an interlaboratory comparison, two Hekla lavas whose V isotopic composition has been reported in ref. 14 were also analyzed in this study.

Results

All vanadium isotope values are reported in standard delta notation $\delta^{51}V_{AA}(‰) = {}^{51/50}V_{sample} / {}^{51/50}V_{AA} - 1$, where AA (Alfa Aesar) is the recognized V standard solution; for brevity we use $\delta^{51}V$ in the text and figures). The $\delta^{51}V$ values of igneous rocks having Fe# (i.e., the molar ratio of $100*FeO_T/(MgO+FeO_T)$, where the subscript "T" indicates all Fe is shown as FeO) similar to mafic rocks in Archean greenstone belts (*SI Appendix*, Fig. S2 and explanation in *Discussion*) show linear increases with differentiation, as tracked by increasing SiO_2 or decreasing MgO (Fig. 1 and *SI Appendix*, Table S1). By contrast, the $\delta^{51}V$ values of high Fe# tholeiites from Hekla and the Anatahan arc also increase linearly with differentiation, but record much steeper trends. Of the two reanalyzed Hekla samples, the $\delta^{51}V$ value of the lower SiO_2 lava is reproduced within uncertainty (Fig. 1), whereas $\delta^{51}V$ for the higher SiO_2 sample is lower than the original published value (14), but the sample still lies significantly above the trend defined by the arc and Kilauea Iki data (Fig. 1), indicating that these Fe-rich lavas have anomalously high $\delta^{51}V$.

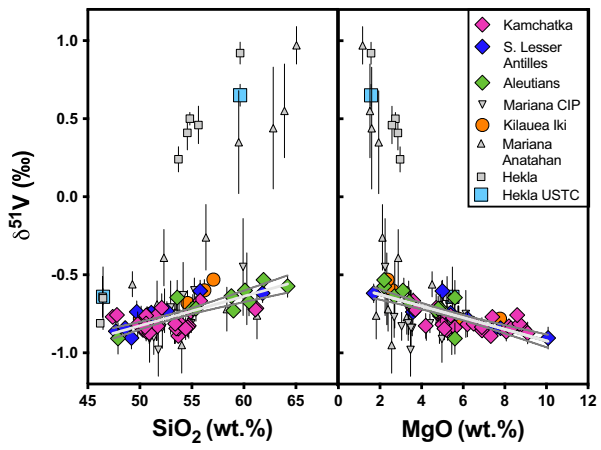

Fig. 1. Correlations between V isotopes in igneous rocks with SiO_2 and MgO (wt.%). $\delta^{51}V$ defines two correlations with SiO_2 and MgO: $\delta^{51}V = SiO_2*(0.016 \pm 0.002) + (-1.611 \pm 0.125)$ and $\delta^{51}V = (-0.037 \pm 0.004) * MgO + (-0.552 \pm 0.024)$. Gray lines represent 95% CI of the linear regressions through the data. Kilauea Iki data are from ref. 17. Gray symbols are previously published data. Larger colored symbols are from this study. Hekla and Mariana data are from ref. 14; two Hekla samples were reproduced here (blue squares). Major element data for Kamchatka, S. Lesser Antilles, and Aleutian samples come from refs. (38–40).

The glacial diamictites show a clear secular evolution in their V isotopic composition, with Mesoarchean samples (~3 Ga) having similar $\delta^{51}V$ values (average value = −0.84‰ ± 0.12‰, two SD, n = 4) to modern mid-ocean ridge basalts (MORBs, average of −0.84‰ ± 0.10‰, two SD, n = 22) (16) and primitive oceanic island basalts (OIBs, average of −0.81‰ ± 0.17‰, two SD, n = 8) (17), whereas the Neoproterozoic and Paleozoic glacial diamictites exhibit elevated $\delta^{51}V$ values from −0.73‰ to −0.54‰; Paleoproterozoic samples fall in between these two groups (Fig. 2 and *SI Appendix*, Table S2).

The range in $\delta^{51}V$ of the magmatic rocks and glacial diamictites in this study (0.38‰ and 0.36‰, respectively) is similar to that observed in differentiated lavas from mid-ocean ridges (~0.3‰) (16), oceanic islands (Kilauea Iki, Hawaii, ~0.4‰) (17), and calc-alkaline lavas from the Central Island Province of the Mariana Arc (14), but significantly smaller than those reported for the Fe-rich lavas from Anatahan, Mariana island arc, and the Hekla volcano in Iceland (14) (*SI Appendix*, Supplementary Text-SOM.4).

Discussion

The combined data for OIB, MORB, and arc lavas show that $\delta^{51}V$ of the fractionating melt increases linearly with crystallization of silicate minerals and magnetite (14, 16, 17). However, tholeiitic lavas from Anatahan Island (Northern Mariana Arc) and Hekla Volcano (Iceland) (*SI Appendix*, Fig. S3), which have significantly higher Fe# than nearly all igneous rocks from Archean greenstone belts (*SI Appendix*, Fig. S2) as well as the tholeiitic Kilauea Iki samples, evolve to much higher $\delta^{51}V$ (Fe#s of the primary magma of Kilauea Iki, Hekla and Anatahan are 51.3, 74.3, and 68.0, respectively, see *SI Appendix*, Dataset S2). The difference is also reflected in the calculated V isotope fractionation factors, with a $\Delta^{51}V_{mineral-melt}$ value of ~ −0.4 to −0.5‰ for Hekla and Anatahan lavas compared with −0.1 to −0.15‰ for Kilauea Iki lavas (14, 17). These differences are likely due to the amount of magnetite, and timing of magnetite saturation, which is greatly influenced by the parental magma composition, as discussed in ref. 17. Parental magmas that are unusually enriched in FeO and thus have high Fe# fractionate a large amount of magnetite (41–44) (*SI Appendix*, Supplementary Text-SOM.4), leading to significant V isotope fractionation. Moreover, Hekla and Anatahan tholeiitic lavas are characterized by extreme Fe enrichment in their parental magmas (Fe# of 74.3 for Hekla and 68.0 for Anatahan, data in *SI Appendix*, Dataset S2) and maintain high Fe# throughout differentiation and, thus, through the variation in SiO_2 (*SI Appendix*, Fig. S2). By contrast, Archean greenstone belt lavas, along with tholeiitic Kilauea Iki samples and modern subduction zone magmas other than Anatahan, start with much lower Fe# and show continuously rising trends in Fe# during differentiation (*SI Appendix*, Fig. S2). Although Francis et al. (45) and Gibson (46) document the existence of Fe-rich melts in the Archean (45, 46), such melts also have high MgO contents and their average Fe# is not elevated (*SI Appendix*, Fig. S2). Thus, magmatic differentiates whose parental magmas have comparable Fe# to Archean greenstone belt lavas should provide a better analog for V isotope behavior during Archean igneous differentiation and continental crust formation.

Because both subduction zone and intraplate lavas can generate intermediate and felsic igneous rocks, and both may have contributed to growth of continental crust (2, 3, 47, 48), we use the samples that do not show evidence for excessive magnetite crystallization to

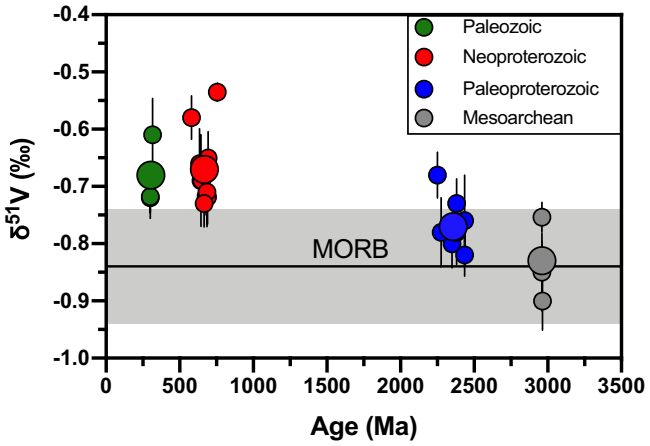

Fig. 2. The $\delta^{51}V$ in diamictite composites as a function of depositional age. Smaller solid circles are individual composites with error bars representing two SD, and larger symbols are the average values of the composites from the same time period. The depositional ages are from ref. 26. The gray band and solid horizontal line denote the $\delta^{51}V$ range and average of mid-ocean ridge basalts (MORBs), respectively; MORB data are from ref. 16.

define the V isotope fractionation trajectory operative during the formation of continental crust. This includes calc-alkaline arc lavas from Kamchatka, Southern Lesser Antilles, the Aleutians, and tholeiitic intraplate samples with normal Fe# from Kilauea Iki, Hawai'i. Moreover, V isotope fractionation is not affected by a change in the degree of mantle melting that would result from secular mantle cooling (*SI Appendix*, Supplementary Text-SOM.7). Therefore, V isotopic fractionation during magmatic differentiation based on modern igneous samples can be applied to Archean rocks.

Although the provenance of the ancient glacial diamictites includes chemically weathered regolith (25–27), the secular evolution of $\delta^{51}V$ in the diamictites is not influenced by alteration or chemical weathering processes. This is because V isotopes are immune to alteration and chemical weathering influences (*SI Appendix*, Supplementary Text-SOM.8), as shown by the similarity of $\delta^{51}V$ among laterites, highly altered basalts, peridotites, picrites, or komatiites and their pristine equivalents (16, 49–51). Moreover, diamictites are, by definition, unsorted sedimentary rocks; so mineral sorting will not influence their composition. Finally, although Fe-oxides (magnetite or hematite) are present as detrital phases in some of the diamictites based on X-ray diffraction data (52), the $\delta^{51}V$ in these samples is not different from other samples of the same age (e.g., compare Mozaan with 7% magnetite to other Mesoarchean samples with no detectable Fe-oxides). Thus, glacial diamictites represent the composites of detrital materials physically eroded from exposed crust, and our results suggest that the emergent UCC evolved to heavier V isotopic compositions after the Mesoarchean (~3 Ga onward).

Integrating the $\delta^{51}V$-SiO_2-MgO systematics of magmatic rocks with the results for the glacial diamictite composites, the progressive enrichment of heavy V isotope in ancient glacial diamictites through time reflects enhanced contribution of felsic rocks in the UCC starting at ~2.4 Ga (Fig. 3 and *SI Appendix*, Fig. S5). Using the tight positive correlations between $\delta^{51}V$ values and SiO_2 contents [$\delta^{51}V = SiO_2*(0.016 \pm 0.002) + (-1.611 \pm 0.125)$] and negative correlations with MgO contents [$\delta^{51}V = (-0.037 \pm 0.004) * MgO + (-0.552 \pm 0.024)$], the range of $\delta^{51}V$ values between −0.73‰ and −0.54‰ for the ≤~2.4 Ga glacial diamictites requires significant proportions of felsic rocks in their provenances.

We estimate the relative proportions of felsic (granite), mafic (basalt), and ultramafic (komatiite) end members in the UCC over time (*SI Appendix*, Fig. S5 and Supplementary Text-SOM.6) using the inferred SiO_2 contents of the UCC at different periods and a ternary (granite-basalt-komatiite) or binary (granite-basalt) mixing model (*SI Appendix*, Fig. S5). In the ternary model, Ni/Co is used as an additional constraint to determine the proportion of komatiite because OIB, MORB, subduction zone basalts, and komatiite have similar $\delta^{51}V$ values within analytical error, while komatiites are characterized by high Ni/Co compared with mafic and felsic rocks (*SI Appendix*, Table S3). According to our calculations, the proportion of basalt decreased from 87 ± 2 wt.% at ~2.9 Ga, through 84 ± 11 wt.% at ~2.3 Ga to ~55 ± 12 wt.% at ~0.6 Ga and ~0.3 Ga, while the proportion of granites (sensu lato) increased from 0 ± 17 wt.% at ~2.9 Ga, through 16 ± 11 wt.% at ~2.3 Ga to 45 ± 12 wt.% at ~0.6 Ga and ~0.3 Ga, offsetting the contribution from komatiite, which significantly decreased following the Archean (i.e., 13 ± 2.0 wt.% at ~2.9 Ga, to negligible after ~2.3 Ga) (*SI Appendix*, Table S4). This decreasing komatiite fraction is consistent with the fact that ultramafic lavas are mostly found in the Archean and almost disappear after 3 Ga (53).

The reconstructed UCC composition through time shows that the transition from mafic to more felsic crust occurred after ~2.9 Ga. The debate regarding the temporal evolution of the composition of UCC rests on two divergent conclusions on the nature of Archean UCC. Trace element ratio or concentration systematics (e.g., Ni/Co, Cr/Zn in terrigenous sediments, normalized Cu concentrations for UCC in glacial diamitites, and

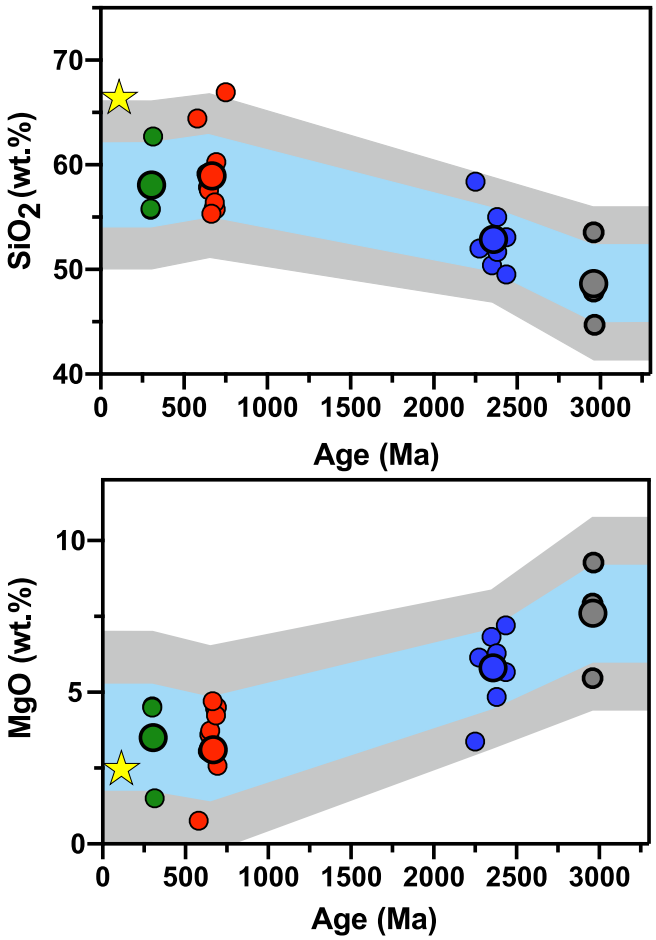

Fig. 3. Temporal variation in SiO_2 and MgO contents of the upper continental crust, calculated from the V isotope ratios of the diamictites (Fig. 2) and the change in $\delta^{51}V$ as a function of differentiation (Fig. 1). The smaller and larger circles represent individual and average values, respectively. The blue and gray areas denote the uncertainty of one and two SDs, respectively. The yellow stars represent a present-day UCC estimate from ref. 1.

Cr/U in shales) indicate that the Archean UCC was dominated by mafic rocks and that the UCC evolved toward a more felsic bulk composition around 2.7 to 2.2 Ga. A Rb/Sr model, which was applied to reconstruct juvenile continental crust, supports this conclusion (9). However, the evidence from other element ratios, such as Al_2O_3/TiO_2, Ni/TiO_2, Sc/Zr, has been interpreted to indicate that that the Archean UCC was more felsic (~56 wt.% SiO_2), and evolved toward a more differentiated composition until reaching the composition of present-day UCC (7, 8), which was supported by Ti isotopic and Sm-Nd isotopic studies (2, 13). The V isotope data presented here for the glacial diamitites clearly show that mafic lithologies were a major component of the Mesoarchean UCC, consistent with the view that a profound compositional transformation occurred globally after 3 Ga.

Secular evolution of the composition of the UCC has implications for the feedback between the onset of plate tectonics, accumulation of O_2 in the atmosphere and ocean, and nutrient supply to the oceans. Estimates for the timing of initiation of plate tectonics range from early Hadean to ~0.85 Ga based on many different lines of evidence (54, 55). Difficulties in determining this timing mainly arise from the fragmentary rock record for the early Earth and debate on the tectonic setting (subduction or non-subduction) of Archean tonalite–trondhjemite–granodiorite (TTG) suites (56–59). Regardless of the TTG formation mechanism, the globally synchronous occurrence of intermediate-felsic crust must be catalyzed by subduction of water into the mantle, which is greatly facilitated by subduction (60–62). Therefore, the compositional change in UCC from a dominantly mafic to a more intermediate or felsic composition may mark the onset of global plate tectonics, indicating global plate tectonics initiated either since the early Archean, or, at the end of Archean (~2.9 to 2.2 Ga) (2, 3, 7, 12). Our findings support the view that global plate tectonics probably had not started earlier than 2.9 Ga. Furthermore, recycling of surface materials into the mantle is a direct consequence of subduction. Inert noble gas systematics serve as a tracer of atmospheric input to the mantle. Recent Xe isotopic studies indicate that effective recycling of Xe and likely other volatile components could not have occurred before 2.8 Ga, which supports a late Archean start of global plate tectonics (63, 64). Other lines of evidence, such as geological records that indicate the strength of the crust, the thermal conditions recorded in metamorphic rocks, the changing rates of crustal growth due to recycling (55), temporal thermal evolution of the mantle (65, 66), and the $\delta^{18}O$ of igneous zircon from the well-preserved Pilbara Craton (67) also agree with the constraints inferred from the V isotopic data.

Mafic lithologies naturally suppress the accumulation of O_2 because they are enriched in the reductants Fe^{2+} and S^{2-}. Serpentinization of mafic to ultramafic rocks also scavenges O_2 (5, 10). The Great Oxidation Event, manifested as an increase in atmospheric partial pressure of free oxygen from <2 ppm to a few percent 2.4 to 2.2 Ga ago, may have been a response, in part, to the transition from mafic to felsic continental crust at the end of Archean (5). In addition, the decline in the proportion of mafic rocks in the UCC, accumulation of organic matter and O_2 in the oceans, and rapid expansion of subaerial crust have approximately coincided at 3.0 to 2.5 Ga ago (68–70). The UCC composition and emerged land area control the influx of important limiting nutrients into oceans such as nickel and phosphorus, which show a decrease and an increase, respectively, at the Archean-Proterozoic boundary (~2.5 Ga). A high Ni flux leads to a high biogenic CH_4 production, whereas enhanced phosphorus flux should accelerate rates of oxygen production (6, 30). Thus, the change in the weathering flux of nickel and phosphorus from continents to oceans in the late Archean may have initiated a positive feedback leading to a persistent oxygenation of atmosphere and oceans (6, 30). Collectively, our V isotopic data and model for reconstruction of the secular evolution of Earth's upper continental crust composition, and by inference, timing of onset of global plate tectonics, provide important insights into the changing habitability of Earth.

Methods summary

Sample powders containing 6 to 10-μg V were dissolved in a 3:1 (v/v) mixture of concentrated hydrofluoric acid and nitric acid. The samples were purified using the ion-exchange chromatography method (71). The total procedural V blank was 1 to 2 ng, which is negligible compared with the total amount of V processed. The recovery rates of the purification procedures were higher than 99%.

Vanadium isotopic ratios were measured on a Thermo-Fisher Scientific MC-ICP-MS (Neptune Plus) at USTC. The effects of mass fractionation were corrected using a sample-standard bracketing method. ^{49}Ti and ^{53}Cr were simultaneously measured to correct for isobaric interferences from ^{50}Ti and ^{50}Cr, respectively. The long-term reproducibility of $\delta^{51}V$ was better than 0.08‰ (two SD) based on repeat analyses of standards (BDH, USTC-V, and NIST-3165). The $\delta^{51}V$ for USGS rock standards determined in the course of this study were BCR-2 (–0.83 ± 0.08‰, two SD, n = 3), BHVO-2 (–0.87 ± 0.09‰, two SD, n = 3), AGV-2 (–0.71 ± 0.04‰, two SD, n = 3), and SGR-1 (–0.15 ± 0.06‰, two SD, n = 3). Replicates of samples (KOM-06, RB030382, KEJ100, Bolivia, Makganyene, Coronation) show excellent reproducibility within the analytical errors.

Mixing models were employed to calculate the contribution of three end members with felsic, mafic, and komatiitic components to the temporal variations of the continental crust. The contents of SiO_2 wt.% and the ratio of Ni/Co were used to solve the mixing equations. A full description of the methods employed are available in the *SI Appendix*, Supplementary Text-SOM of the online version of this manuscript.

Data, Materials, and Software Availability. All study data are included in the article and/or supporting information.

ACKNOWLEDGMENTS. This study was supported by National Natural Science Foundation of China (41630206, 41325011) and the Strategic Priority Research Program (B) of Chinese Academy of Sciences (Grant No. XDB18000000) to F.H. Funding for study of the diamictites was provided by NSF grant EAR-1321954 to R.M.G. and R.L.R. We thank Haraldur Sigurdsson and Gerhard Wörner for providing subduction zone samples and J.P. for providing Hekla samples. Zhengbin Deng and Lu Pan are thanked for their constructive comments on improving the manuscript. The paper benefitted from thorough reviews by P.A.C. and J.P.

Author affiliations: [a]Chinese Academy of Sciences, Key Laboratory of Crust-Mantle Materials and Environments, School of Earth and Space Sciences, University of Science and Technology of China, Anhui 230026, China; [b]Chinese Academy of Sciences, Center for Excellence in Comparative Planetology, University of Science and Technology of China, Hefei 230026, China; [c]School of Earth Sciences, State Key Laboratory of Geological Processes and Mineral Resources, China University of Geosciences, Wuhan 430074, China; [d]State Key Laboratory of Palaeobiology and Stratigraphy, Nanjing Institute of Geology and Palaeontology, Nanjing 210008, China; [e]Center for Excellence in Life and Paleoenvironment, Chinese Academy of Sciences, Nanjing 210008, China; [f]Department of Environmental, Earth and Atmospheric Sciences, University of Massachusetts Lowell, Lowell, MA 01854; [g]Department of Earth Science, University of California–Santa Barbara, Santa Barbara, CA 93106; and [h]Earth Research Institution, University of California-Santa Barbara, Santa Barbara, CA 93106

1. R. L. Rudnick, S. Gao, "The Composition of the Continental Crust" in *The Crust*, H. D. Holland and K. K. Turekian, Eds. (Elsevier-Pergamon, Oxford, UK, 2014), **vol. 4**, pp. 1–51.
2. N. D. Greber *et al.*, Titanium isotopic evidence for felsic crust and plate tectonics 3.5 billion years ago. *Science* **357**, 1271–1274 (2017).
3. M. Tang, K. Chen, R. L. Rudnick, Archean upper crust transition from mafic to felsic marks the onset of plate tectonics. *Science* **351**, 372–375 (2016).
4. J. F. Kasting, D. Catling, Evolution of a habitable planet. *Annu. Rev. Astron. Astrophys.* **41**, 429–463 (2003).
5. C.-T.A. Lee *et al.*, Two-step rise of atmospheric oxygen linked to the growth of continents. *Nat. Geosci.* **9**, 417–424 (2016).
6. L. J. Alcott, B. J. Mills, A. Bekker, S. W. Poulton, Earth's great oxidation event facilitated by the rise of sedimentary phosphorus recycling. *Nat. Geosci.* **15**, 210–215 (2022).
7. M. P. Ptáček, N. Dauphas, N. D. Greber, Chemical evolution of the continental crust from a data-driven inversion of terrigenous sediment compositions. *Earth Planet. Sci. Lett* **539**, 116090 (2020).
8. N. D. Greber, N. Dauphas, The chemistry of fine-grained terrigenous sediments reveals a chemically evolved Paleoarchean emerged crust. *Geochim. Cosmochim. Acta* **255**, 247–264 (2019).
9. B. Dhuime, A. Wuestefeld, C. J. Hawkesworth, Emergence of modern continental crust about 3 billion years ago. *Nat. Geosci.* **8**, 552–555 (2015).
10. M. A. Smit, K. Mezger, Earth's early O2 cycle suppressed by primitive continents. *Nat. Geosci.* **10**, 788 (2017).
11. R. Large *et al.*, Role of upper-most crustal composition in the evolution of the Precambrian ocean–atmosphere system. *Earth Planet. Sci. Lett.* **487**, 44–53 (2018).
12. K. Chen *et al.*, How mafic was the Archean upper continental crust? Insights from Cu and Ag in ancient glacial diamictites. *Geochim. Cosmochim. Acta* **278**, 16–29 (2020).
13. M. Garçon, Episodic growth of felsic continents in the past 3.7 Ga. *Sci. Adv.* **7**, eabj1807 (2021).
14. J. Prytulak *et al.*, Stable vanadium isotopes as a redox proxy in magmatic systems? *Geochem. Perspect. Lett.* **3**, 75–84 (2017).
15. P. A. Sossi, J. Prytulak, H. S. C. O'Neill, Experimental calibration of vanadium partitioning and stable isotope fractionation between hydrous granitic melt and magnetite at 800 °C and 0.5 GPa. *Contrib. Mineral. Petrol.* **173**, 27 (2018).
16. F. Wu *et al.*, Vanadium isotope compositions of mid-ocean ridge lavas and altered oceanic crust. *Earth Planet. Sci. Lett.* **493**, 128–139 (2018).
17. X. Ding, R. T. Helz, Y. Qi, F. Huang, Vanadium isotope fractionation during differentiation of Kilauea Iki lava lake, Hawaii. *Geochim. Cosmochim. Acta* **289**, 114–129 (2020).
18. G. Mallmann, H. S. C. O'Neill, The crystal/melt partitioning of V during mantle melting as a function of oxygen fugacity compared with some other elements (Al, P, Ca, Sc, Ti, Cr, Fe, Ga, Y, Zr and Nb). *J. Petrol.* **50**, 1765–1794 (2009).
19. S. Sutton *et al.*, Vanadium K edge XANES of synthetic and natural basaltic glasses and application to microscale oxygen barometry. *Geochim. Cosmochim. Acta* **69**, 2333–2348 (2005).
20. M. J. Toplis, A. Corgne, An experimental study of element partitioning between magnetite, clinopyroxene and iron-bearing silicate liquids with particular emphasis on vanadium. *Contrib. Mineral. Petrol.* **144**, 22–37 (2002).
21. Z. Deng *et al.*, Titanium isotopes as a tracer for the plume or island arc affinity of felsic rocks. *Proc. Natl. Acad. Sci. U.S.A.* **116**, 1132–1135 (2019).
22. A. C. Johnson *et al.*, Titanium isotopic fractionation in Kilauea Iki lava lake driven by oxide crystallization. *Geochim. Cosmochim. Acta* **264**, 180–190 (2019).
23. X. Zhao *et al.*, Titanium isotopic fractionation during magmatic differentiation. *Contrib. Mineral. Petrol.* **175**, 67 (2020).
24. L. Hoare *et al.*, Melt chemistry and redox conditions control titanium isotope fractionation during magmatic differentiation. *Geochim. Cosmochim. Acta* **282**, 38–54 (2020).
25. R. M. Gaschnig *et al.*, Compositional evolution of the upper continental crust through time, as constrained by ancient glacial diamictites. *Geochim. Cosmochim. Acta* **186**, 316–343 (2016).
26. A. T. Greaney *et al.*, Molybdenum isotope fractionation in glacial diamictites tracks the onset of oxidative weathering of the continental crust. *Earth Planet. Sci. Lett* **534**, 116083 (2020).
27. S. Li, R. M. Gaschnig, R. L. Rudnick, Insights into chemical weathering of the upper continental crust from the geochemistry of ancient glacial diamictites. *Geochim. Cosmochim. Acta* **176**, 96–117 (2016).
28. A. Mundl, R. J. Walker, J. R. Reimink, R. L. Rudnick, R. M. Gaschnig, Tungsten-182 in the upper continental crust: Evidence from glacial diamictites. *Chem. Geol.* **494**, 144–152 (2018).
29. X. Y. Nan *et al.*, Barium isotopic composition of the upper continental crust. *Geochim. Cosmochim. Acta* **233**, 33–49 (2018).
30. S.-J. Wang, R. L. Rudnick, R. M. Gaschnig, H. Wang, L. E. Wasylenki, Methanogenesis sustained by sulfide weathering during the Great Oxidation Event. *Nat. Geosci.* **12**, 296 (2019).
31. S. Tian *et al.*, Zirconium isotopic composition of the upper continental crust through time. *Earth Planet. Sci. Lett.* **572**, 117086 (2021).
32. X. M. Liu, R. M. Gaschnig, R. L. Rudnick, R. M. Hazen, A. Shahar, Constant iron isotope composition of the upper continental crust over the past 3 Gyr. *Geochem. Perspect. Lett.* **22**, 16–19 (2022).
33. S. Li *et al.*, Molybdenum contents of sulfides in ancient glacial diamictites: Implications for molybdenum delivery to the oceans prior to the Great Oxidation Event. *Geochim. Cosmochim. Acta* **278**, 30–50 (2020).
34. R. M. Gaschnig, M. F. Horan, R. L. Rudnick, J. D. Vervoort, C. M. Fisher, History of crustal growth in Africa and the Americas from detrital zircon and Nd isotopes in glacial diamictites. *Precambrian Res.* **373**, 106641 (2022).
35. K. Chen *et al.*, Platinum-group element abundances and Re–Os isotopic systematics of the upper continental crust through time: Evidence from glacial diamictites. *Geochim. Cosmochim. Acta* **191**, 1–16 (2016).
36. M. E. Murphy *et al.*, Homogenising the upper continental crust: The Si isotope evolution of the crust recorded by ancient glacial diamictites. *Earth Planet. Sci. Lett.* **591**, 117620 (2022).
37. R. M. Gaschnig *et al.*, Onset of oxidative weathering of continents recorded in the geochemistry of ancient glacial diamictites. *Earth Planet. Sci. Lett.* **408**, 87–99 (2014).
38. T. Churikova, F. Dorendorf, G. WÖRner, Sources and fluids in the mantle wedge below Kamchatka, evidence from across-arc geochemical variation. *J. Petrol.* **42**, 1567–1593 (2001).
39. F. Huang, C. C. Lundstrom, H. Sigurdsson, Z. Zhang, U-series disequilibria in Kick'em Jenny submarine volcano lavas: A new view of time-scales of magmatism in convergent margins. *Geochim. Cosmochim. Acta* **75**, 195–212 (2011).
40. Y. Cai *et al.*, Distinctly different parental magmas for calc-alkaline plutons and tholeiitic lavas in the central and eastern Aleutian arc. *Earth Planet. Sci. Lett.* **431**, 119–126 (2015).
41. R. Arató, A. Audétat, FeTiMM–A new oxybarometer for mafic to felsic magmas. *Geochem. Perspect. Lett.* **5**, 19–23 (2017).
42. R. H. Nandedkar, P. Ulmer, O. Müntener, Fractional crystallization of primitive, hydrous arc magmas: An experimental study at 0.7 GPa. *Contrib. Mineral. Petrol.* **167**, 1015 (2014).
43. P. Ulmer, R. Kaegi, O. Müntener, Experimentally derived intermediate to silica-rich arc magmas by fractional and equilibrium crystallization at 1·0 GPa: An evaluation of phase relationships, compositions, liquid lines of descent and oxygen fugacity. *J. Petrol.* **59**, 11–58 (2018).
44. Z. Deng *et al.*, Early oxidation of the martian crust triggered by impacts. *Sci. Adv.* **6**, eabc4941 (2020).
45. D. Francis, J. Ludden, R. Johnstone, W. Davis, Picrite evidence for more Fe in Archean mantle reservoirs. *Earth Planet. Sci. Lett.* **167**, 197–213 (1999).
46. S. A. Gibson, Major element heterogeneity in Archean to recent mantle plume starting-heads. *Earth Planet. Sci. Lett.* **195**, 59–74 (2002).
47. I. H. Campbell, D. R. Davies, Raising the continental crust. *Earth Planet. Sci. Lett.* **460**, 112–122 (2017).
48. M. Willbold, E. Hegner, A. Stracke, A. Rocholl, Continental geochemical signatures in dacites from Iceland and implications for models of early Archaean crust formation. *Earth Planet. Sci. Lett.* **279**, 44–52 (2009).
49. J. Prytulak *et al.*, The stable vanadium isotope composition of the mantle and mafic lavas. *Earth Planet. Sci. Lett.* **365**, 177–189 (2013).
50. Y.-H. Qi *et al.*, Vanadium isotope composition of the Bulk Silicate Earth: Constraints from peridotites and komatiites. *Geochim. Cosmochim. Acta* **259**, 288–301 (2019).
51. Y.-H. Qi *et al.*, Coupled variations in V-Fe abundances and isotope compositions in latosols: Implications for V mobilization during chemical weathering. *Geochim. Cosmochim. Acta* **320**, 26–40 (2022).
52. P.-Y. Han *et al.*, Halogen (F, Cl, Br, and I) concentrations of the upper continental crust through time as recorded in ancient glacial diamictite composites. *Geochim. Cosmochim. Acta* **341**, 28–45 (2023).
53. N. Arndt, C. Lesher, S. Barnes, *Komatiite* (Cambridge University Press, 2008), p. 458.
54. J. Korenaga, Initiation and evolution of plate tectonics on earth: Theories and observations. *Annu. Rev. Earth Planet. Sci.* **41**, 117–151 (2013).
55. C. Hawkesworth, P. A. Cawood, B. Dhuime, The evolution of the continental crust and the onset of plate tectonics. *Front. Earth Sci. (Lausanne)* **8**, 326 (2020).
56. M. A. Smit *et al.*, Formation of Archean continental crust constrained by boron isotopes. *Geochem. Perspect. Lett.* **12**, 23–26 (2019), 10.7185/geochemlet.1930.
57. Z. Deng *et al.*, An oceanic subduction origin for Archaean granitoids revealed by silicon isotopes. *Nat. Geosci.* **12**, 774–778 (2019).
58. S. Foley, M. Tiepolo, R. Vannucci, Growth of early continent crust controlled by melting of amphibolite in subduction zones. *Nature* **417**, 837–840 (2002).
59. R. L. Rudnick, Making continental crust. *Nature* **378**, 571 (1995).
60. J. Korenaga, Plate tectonics and planetary habitability: Current status and future challenges. *Ann. N. Y. Acad. Sci.* **1260**, 87–94 (2012).
61. I. H. Campbell, S. R. Taylor, No water, no granite–No oceans, no continents. *Geophys. Res. Lett.* **10**, 1061–1064 (1983).
62. K. Regenauer-Lieb, D. A. Yuen, J. Branlund, The initiation of subduction: Criticality by addition of water? *Science* **294**, 578–580 (2001).
63. S. Péron, M. Moreira, Onset of volatile recycling into the mantle determined by xenon anomalies. *Geochem. Perspect. Lett.* **9**, 21–25 (2018), 10.7185/geochemlet.1833.
64. R. Parai, S. Mukhopadhyay, Xenon isotopic constraints on the history of volatile recycling into the mantle. *Nature* **560**, 223–227 (2018).
65. S. Labrosse, C. Jaupart, Thermal evolution of the Earth: Secular changes and fluctuations of plate characteristics. *Earth Planet. Sci. Lett.* **260**, 465–481 (2007).
66. M. Brown, T. Johnson, N. J. Gardiner, Plate tectonics and the archean Earth. *Annu. Rev. Earth Planet. Sci.* **48**, 291–320 (2020).
67. T. E. Johnson *et al.*, Giant impacts and the origin and evolution of continents. *Nature* **608**, 330–335 (2022).
68. B. Kendall *et al.*, Pervasive oxygenation along late Archaean ocean margins. *Nat. Geosci.* **3**, 647–652 (2010).
69. T. W. Lyons, C. T. Reinhard, N. J. Planavsky, The rise of oxygen in Earth's early ocean and atmosphere. *Nature* **506**, 307–315 (2014).
70. I. N. Bindeman *et al.*, Rapid emergence of subaerial landmasses and onset of a modern hydrologic cycle 2.5 billion years ago. *Nature* **557**, 545–548 (2018).
71. F. Wu *et al.*, Vanadium isotope measurement by MC-ICP-MS. *Chem. Geol.* **421**, 17–25 (2016).